Available online at www.sciencedirect.com
SCIENCE DIRECT®
Journal of Membrane Science 243 (2004) 203–213
journal of MEMBRANE SCIENCE
www.elsevier.com/locate/memsci

Microsystem technology for high-flux hydrogen separation membranes

F.C. Gielens[a,*], H.D. Tong[b], C.J.M. van Rijn[c], M.A.G. Vorstman[a], J.T.F. Keurentjes[a]

[a] *Process Development Group, Department of Chemical Engineering and Chemistry, Eindhoven University of Technology, P.O. Box 513, 5600 MB Eindhoven, The Netherlands*
[b] *Transducer Science Technology Group, MESA+ Research Institute, University of Twente, P.O. Box 217, 7500 AE Enschede, The Netherlands*
[c] *Aquamarijn Micro Filtration B.V., Beatrixlaan 2, 7255 DB Hengelo, The Netherlands*

Received 28 February 2004; accepted 14 June 2004
Available online 17 August 2004

Abstract

The application of thin hydrogen-selective membranes suffers from the occurrence of pinholes and a significant resistance to mass transfer in the porous support. To overcome these problems, Pd, Pd/Ag and Pd–Ta–Pd membranes with a thickness between 0.5 and 1.2 μm have been deposited on a dense and smooth surface of a silicon wafer. After membrane deposition, the underground has been etched to release the membrane surface for H_2 permeation. Membranes have been prepared with a 1 μm thick microsieve as the support or without support. The prepared membranes have been characterized by the H_2 and He flux as a function of temperature (623–723 K) and feed composition ($0 < pH_2 < 0.83$ bar). The highest H_2 flux, 3.6 mol H_2/(m^2 s), has been found with a microsieve-supported 1 μm thick Pd/Ag membrane at 723 K and 0.83 bar hydrogen partial pressure. The fluxes measured here are approximately one order of magnitude higher than the fluxes reported in the literature for Pd or Pd alloy membranes deposited on porous supports. Moreover, helium could not be detected in the permeate, thus indicating the absence of pinholes.

Keywords: Hydrogen permeation; Palladium; Palladium alloys; Pd–Ta–Pd sandwich; Microsystem technology

1. Introduction

Palladium (Pd) membranes are selective for hydrogen and have been used to produce ultra pure H_2 [1]. In processes like dehydrogenations, steam reforming of methane, or the water gas shift reaction, the application of H_2 selective membranes has also been studied [2,3]. In these processes, the membranes are used [4] to improve the single pass conversion by removing H_2 from the reaction zone [5]. Alternatively, the process conditions can be set milder without a loss in conversion, thus reducing the formation of by-products. The membrane can also be used in hydrogenation reactions as inter-stage H_2 feed to improve the yield [6]. However, application of Pd membranes on a large scale is still expensive, thus requiring a significant cost reduction [7]. Increasing the H_2 flux while maintaining a high selectivity will reduce the required membrane area and therefore the membrane investment costs.

During the past decades, the H_2 flux has already been increased significantly by decreasing the membrane thickness from about 1 mm to micrometers and even sub-micrometers [8]. However, the increase in flux by reducing the membrane thickness has its limits, as sub-micron membranes do have a high flux but poor mechanical strength. Additionally, mass transfer resistances in the gas phase at the retentate side and in the porous support can become limiting factors. Although the specific resistance in the support is relatively low as compared to that of the membrane layer, the H_2 flux can significantly be limited due to the thickness of the support. Moreover, resistances can occur at the interface between the Pd surface and the bulk where H atoms are entering or leaving the bulk Pd, or at the interface of the gas phase and the membrane surface where H_2 dissociates at the feed side and H atoms have to associate at the permeate side [9].

* Corresponding author. Tel.: +31 40 2474956; fax: +31 40 2446104.
E-mail address: f.c.gielens@tue.nl (F.C. Gielens).

0376-7388/$ – see front matter © 2004 Elsevier B.V. All rights reserved.
doi:10.1016/j.memsci.2004.06.021

The reduction of the membrane thickness is not only limited by the mechanical strength, but also by the formation of pinholes during fabrication. To prevent pinhole formation, it has been advised to prepare membranes with a thickness equal to at least three times the diameter of the pores in the top layer of the support [10]. Moreover, as it is well known that ceramic porous supports are seldom defect free, this will also decrease the selectivity of the supported membranes.

In this paper, microsystem technology has been used to increase the hydrogen flux through Pd-based membranes and to prevent the formation of pinholes during membrane fabrication. The fabrication and characterization of three different membrane materials will be presented: pure Pd, Pd/Ag alloy, and Ta coated by Pd, respectively. Each of these membranes has specific advantages and disadvantages. Pd is a simple system to study, but undergoes an α–β phase transition between room temperature and 573 K [11]. Pd/Ag has a higher H_2 permeability than pure Pd; the highest permeability for Pd/Ag at 673 K can be obtained with an alloy composition of 77/23 wt.% Pd/Ag [12]. A disadvantage of Pd/Ag membranes, however, is the decreased Pd content at the surface, which can limit the H_2 flux because of the poorer ability of Ag to dissociate/associate H_2 compared to Pd. A Pd coated membrane consists of a material that is more permeable for H_2 than Pd (and is preferably cheaper). This material is coated at both sides with a thin Pd layer. In this study, we use Ta as the more permeable material [13]. The Pd coating is necessary to allow for the dissociation and association of H_2 at the membrane surface and to prevent oxidation of the Ta surface. The Pd coated Ta membrane is expected to have a better permeance than a Pd/Ag or Pd membrane with the same thickness, but only in a certain temperature range. At low temperatures the surface reaction limits the permeation rate, so that there will be no advantage of the high permeability. At too high temperatures, however, Ta will have a lower H_2 permeability compared to Pd or Pd/Ag due to the negative temperature dependency of the H_2 permeability of Ta.

Membranes have been prepared with a 1 μm thick microsieve as a support [14] or without such a support ('free-hanging'). The microsieve as a membrane support has also been applied by Franz et al. [15].

2. Experimental

2.1. Manufacturing of free-hanging membranes

For all membranes described in this paper a double-side polished silicon substrate with crystallographic cut ⟨1 1 0⟩ served as the basis. These substrates, called wafers, were 350 μm thick and 3 in. in diameter. A 1 μm protective layer of wet-thermally oxidized SiO_2 was deposited on both sides of the wafer (Fig. 1). After precise alignment to the ⟨1 1 1⟩ crystal direction, parallelogram-shaped structures of 25 μm × 1250 μm were imprinted on one of the SiO_2 layers by standard photolithography. The SiO_2 layer was removed at

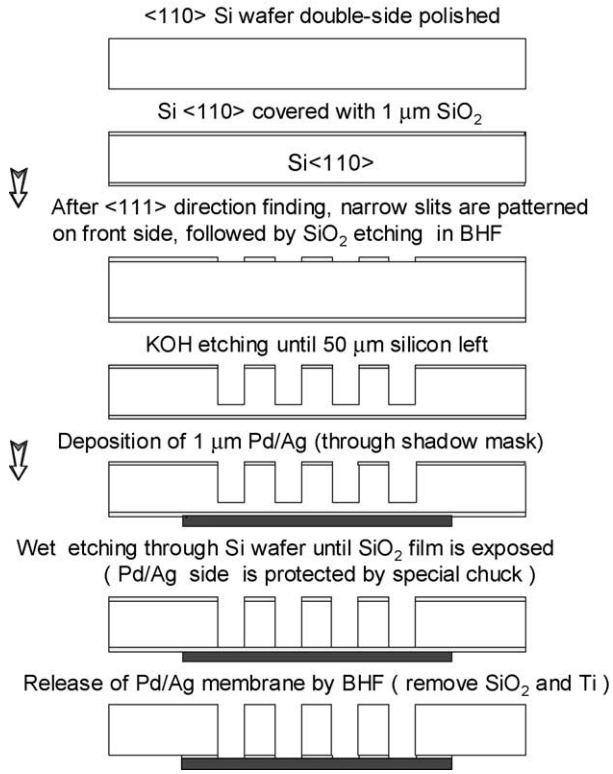

Fig. 1. Schematic view of the followed steps to manufacture a free-hanging membrane.

the imprints with BHF dry etching. When the SiO_2 protection layer was removed, apertures could be etched with KOH inside the wafer. The wet etching was stopped after the apertures reached a depth of 300 μm. A Si layer of 50 μm remained to give sufficient mechanical strength for the next step. Subsequently, the actual membrane, Pd or Pd/Ag alloy, was deposited by (co)-sputtering through a shadow mask on the other side of the wafer, using titanium (Ti) as an adhesion layer. It has to be noted that at this point in the procedure the underground is still closed, which is a large advantage to prevent the formation of pinholes compared to depositing metal layers on top of a porous material as discussed in Section 1. After deposition, the remaining 50 μm silicon is removed with KOH etching, followed by releasing the membrane layer by etching the SiO_2 and Ti layer with BHF. In Fig. 2a, the top view of the aperture side is given; the white part in the middle of the aperture is the Pd (alloy) membrane. In Fig. 2b, a SEM micrograph is given of the cross section of the apertures.

2.2. Manufacturing of microsieve-supported membranes

The manufacturing of the microsieve-supported membranes deviated in some steps from that of the unsupported membrane (Fig. 3). First, a 0.3 μm protective layer of SiO_2 was deposited on both sides of the wafer, followed by a 0.7 μm Si_xN_y layer. Parallelogram-shaped structures of 350 μm × 2100 μm were imprinted on the Si_xN_y layer on one side by standard photolithography. The long side of the

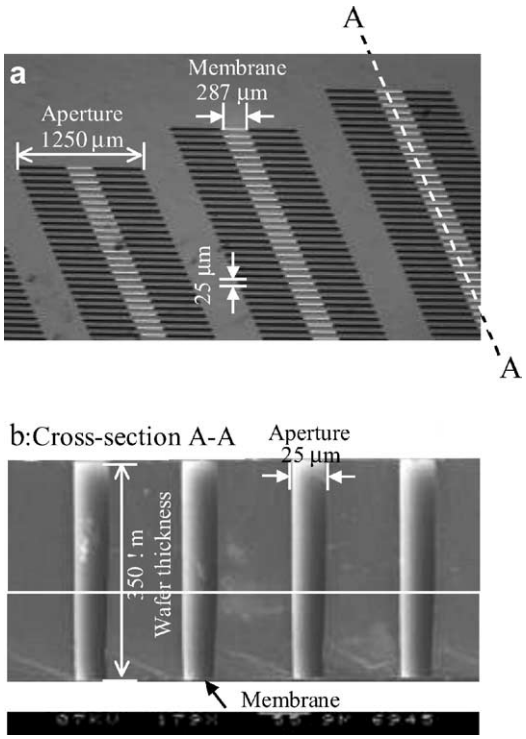

Fig. 2. Two photographs of the free-hanging membrane: (a) top view of the aperture side; (b) SEM picture of the cross section perpendicular to the apertures.

parallelogram was aligned to the ⟨1 1 1⟩ direction of the Si-wafer. The Si_xN_y was removed at the imprints by dry etching (reactive ion etching, RIE). After the SiO_2 protection layer was removed, apertures could be etched with a KOH solution inside the wafer (Fig. 4a). The wet etching was stopped after the apertures reached a depth of 300 μm, again to give enough mechanical strength in the subsequent step. In the remainder of this paper, this side of the wafer will be referred to as 'aperture side', whereas the other side of the wafer will be referred to as 'microsieve side'.

At the other side of the wafer, the microsieve side, a pattern of circular openings of 5 μm in diameter was imprinted on the Si_xN_y layer (Fig. 4b), followed by dry etching of the Si_xN_y layer. The SiO_2 layer was left intact to preserve a closed layer, in order to avoid the formation of pinholes during sputtering of a Pd/Ag layer inside the aperture at the SiO_2 layer of the microsieve in a later step. From the results of van Rijn et al. [16] and the aperture width, it can be expected that the microsieve can withstand a pressure of at least 4 bars. In the next step, the remaining 50 μm Si in the parallelogram-shaped apertures was removed by KOH etching, followed by sputtering of the membrane material onto a surface area of 18 mm × 18 mm at the aperture side (Fig. 4a). Besides the bottom of the aperture (Fig. 4b), which later forms the actual membrane, also the sidewall of the aperture and the wafer area around the aperture were covered by the membrane material during sputtering. Tong et al. [17] showed that a 0.5 μm thick Pd/Ag membrane supported by microsieve can withstand a pressure of 4 bars at room temperature, which is sufficient for industrial applications like the dehydrogenation processes of alkanes and ethylbenzene. Prior to the sputtering of membrane material a Ti layer was sputtered to obtain a good adhesion between the SiO_2 and the membrane layer. In the final step, the SiO_2 and the Ti in the circular openings at the microsieve side were removed with BHF to release the

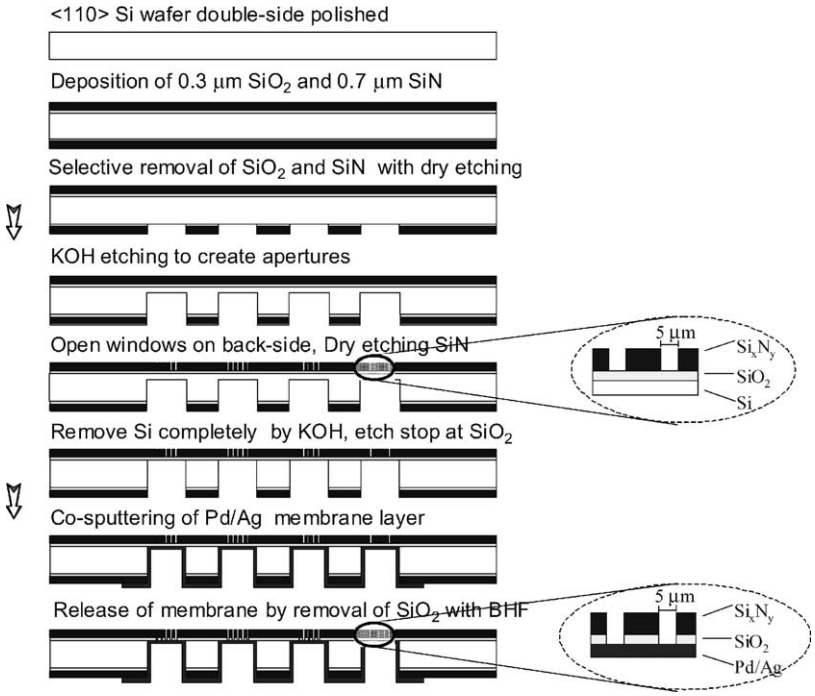

Fig. 3. Schematic view of the followed steps to manufacture a microsieve-supported membrane.

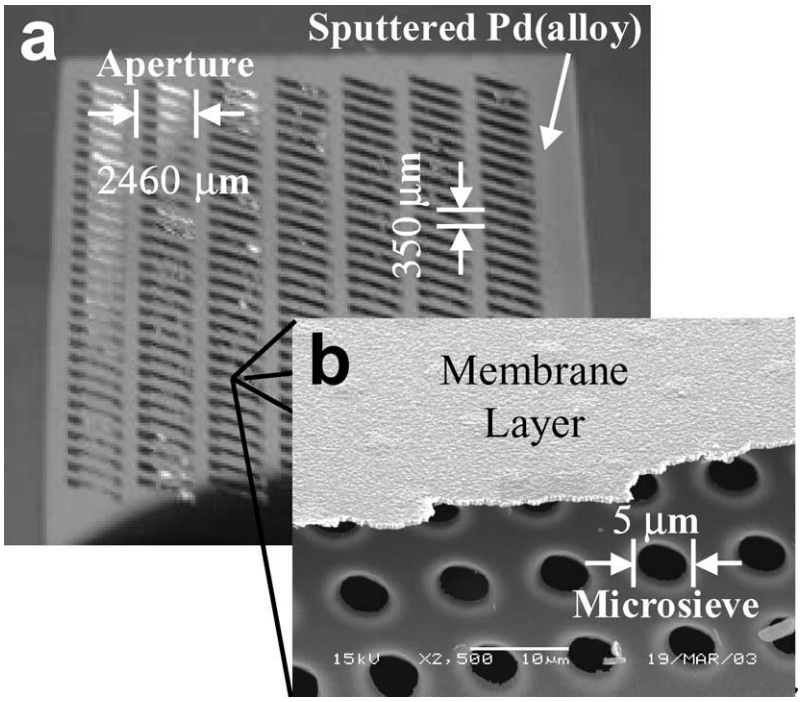

Fig. 4. Two photographs of the microsieve-supported membrane: (a) top view of the aperture side; (b) SEM picture of the membrane layer deposited on top of the microsieve (the membrane layer was partly removed to show the microsieve).

membrane area at the microsieve side. A detailed description of the production of both the free-hanging and microsieve-supported membranes is given by Tong et al. [18–20].

2.3. Metal film deposition

Pd, Ag and Ta targets were used to fabricate the three membrane types that are described in Section 1. The purity of the targets was 99.99 wt.%. The first type of membrane was fabricated by single cannon sputtering of a 1.0 μm Pd layer on top of the SiO_2 layer. The Pd/Ag alloy membrane was fabricated using two ion cannons. The use of two separate ion cannons enables to sputter Pd and Ag simultaneously with a homogeneous Pd/Ag composition as a result. By changing the operating conditions of the two sputter cannons, all possible alloy compositions can be obtained. The Pd/Ag ratio of the membrane was adjusted by using a previously obtained relation between sputtering parameters and final Pd and Ag concentrations. Membranes with alloy compositions close to the optimum of 77/23 wt.% Pd/Ag were made. The thickness of the Pd/Ag membranes was varied from 0.5 to 1.2 μm.

The Pd–Ta–Pd membrane was obtained by sequential sputtering from a Pd and a Ta target. First, a 0.2 μm layer of Pd was sputtered on top of the SiO_2 followed by a 0.6 μm layer of Ta, and finally a 0.2 μm Pd layer was sputtered on top of the Ta layer.

2.4. Module fabrication

A membrane module was developed for laboratory application by bonding the processed Si-wafer between two 5 mm thick borosilicate plates by a four-electrode anodic bonding (Fig. 5). Prior to bonding, two holes were drilled in each glass plate to serve as the inlet and outlet of the gas flow at both sides of the membrane. Additionally, transport ducts were powder blasted in the borosilicate plate to transport the gas from the inlet over the membrane towards the outlet, for which two different designs have been used. In the first design, each glass wafer has one large duct (width 18 mm, length 30 mm, depth 0.2 mm) in which the gas flows over the wafer (Fig. 5). As a consequence, the gas at the aperture side of the membrane has to diffuse through a stagnant layer in the apertures. The effectiveness of H_2 transport can be improved by changing the duct pattern design of the glass plate at the aperture side as in the second design, consisting of four parallel rectangular ducts that are connected to the inlet and five parallel rectangular ducts connected to the outlet (Fig. 6). The two groups of ducts are connected in the module via the apertures in the wafer. This reduces the mass transfer resistance in the gas phase, although at the cost of some additional pressure loss. At the wafer side without apertures the glass plate is identical to the first design. The modules with forced flow trough the slits are referred to as ‘Pd-ff’.

2.5. Characterization of membranes

The Pd/Ag ratio of the membrane was confirmed by measuring a sample by X-ray photoelectron spectroscopy (XPS, Quantum 2000 Scanning ESCA Microprobe). The sample was prepared by sputtering a Pd/Ag layer on a Si wafer at conditions identical to those of the membrane fabrication.

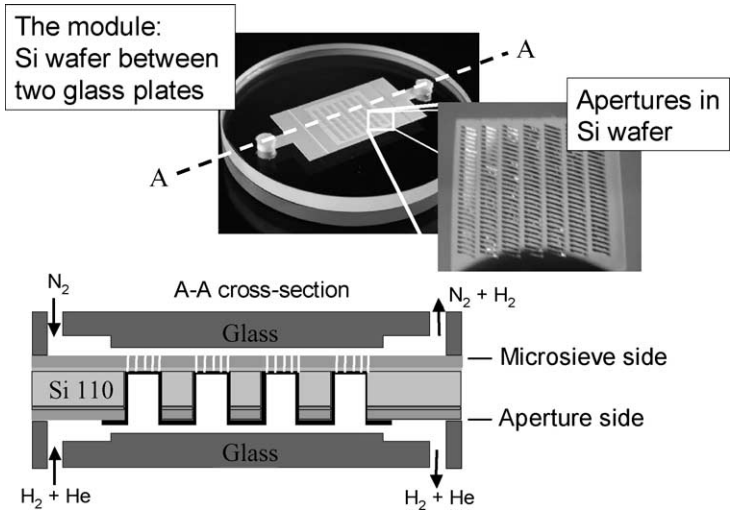

Fig. 5. Photograph and schematic drawing of the membrane module design without a forced gas flow through the slits. The gasses flow over the wafer and H_2 transport to the membrane is mainly based on diffusion.

The Pd/Ag ratio at various depths was also determined with XPS measurements.

The thickness of the membrane was measured using a Dektak surface profiler and scanning electron microscope (SEM, Jeol JSM-5600). The Dektak surface profiler could only measure the thickness of the Pd/Ag layer at the surface of the wafer at the aperture side. However, after breaking the wafer, it was possible to determine the Pd/Ag layer thickness inside the aperture on the microsieve by SEM.

The permeance and selectivity of the membranes were determined using the experimental set-up shown in Fig. 7. The retentate and permeate side were continuously flushed: the retentate side with a known mixture of H_2 and He, and the permeate side with N_2. All gas flows were regulated by mass flow controllers. The retentate and permeate flow rates were varied between 100 and 1000 ml/min. The purity of H_2, He and N_2 was 99.999%. The absolute pressure of the retentate side was controlled by a pressure controller and was set slightly above atmospheric pressure. The trans-membrane pressure was kept below 20 mbar. The permeance and selectivity were determined by measuring the H_2 and He concentration in the N_2 stream by a GC, equipped with a thermal conductivity detector (TCD). More detailed information about the experimental set-up has been given in a previous paper [21].

To investigate the influence of the activation step, three membranes were not activated, while the other membranes were activated for at least 3 h at a temperature of 673 or 723 K, respectively, depending on the operating temperature of the first experiment. During activation, a mixture of 20/80 vol.% H_2/He was fed to both the retentate and permeate side of the membrane. The activation state of the membranes used

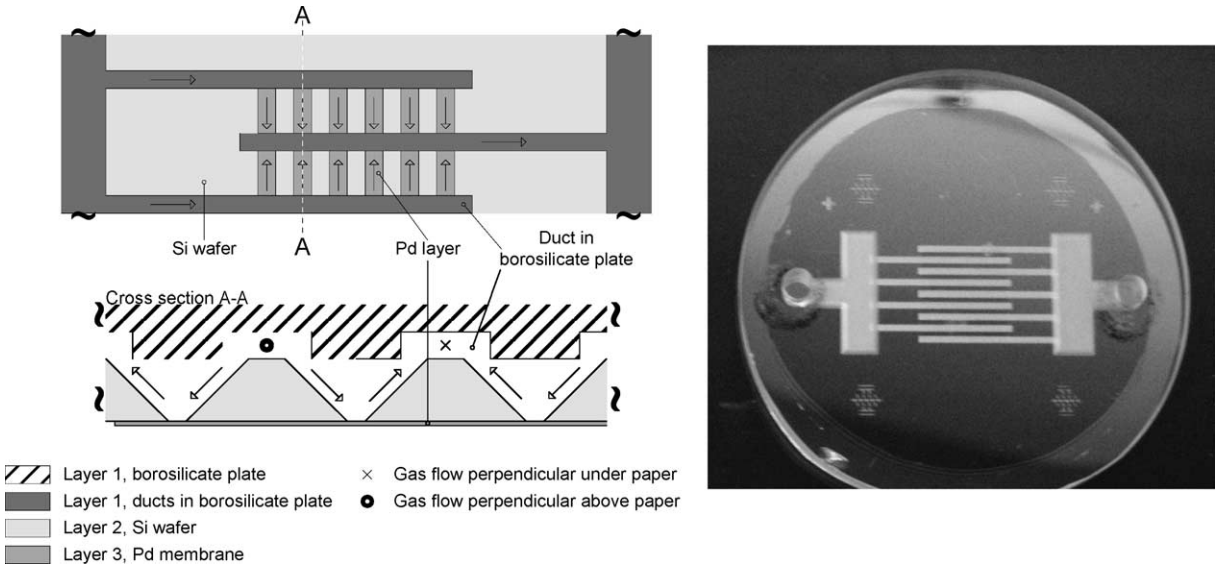

Fig. 6. Photograph and schematic drawing of the membrane module design with a forced gas flow through the slits (ff). The gasses are forced through the apertures in the wafer, which results in a lower mass transfer resistance than in the design shown in Fig. 5.

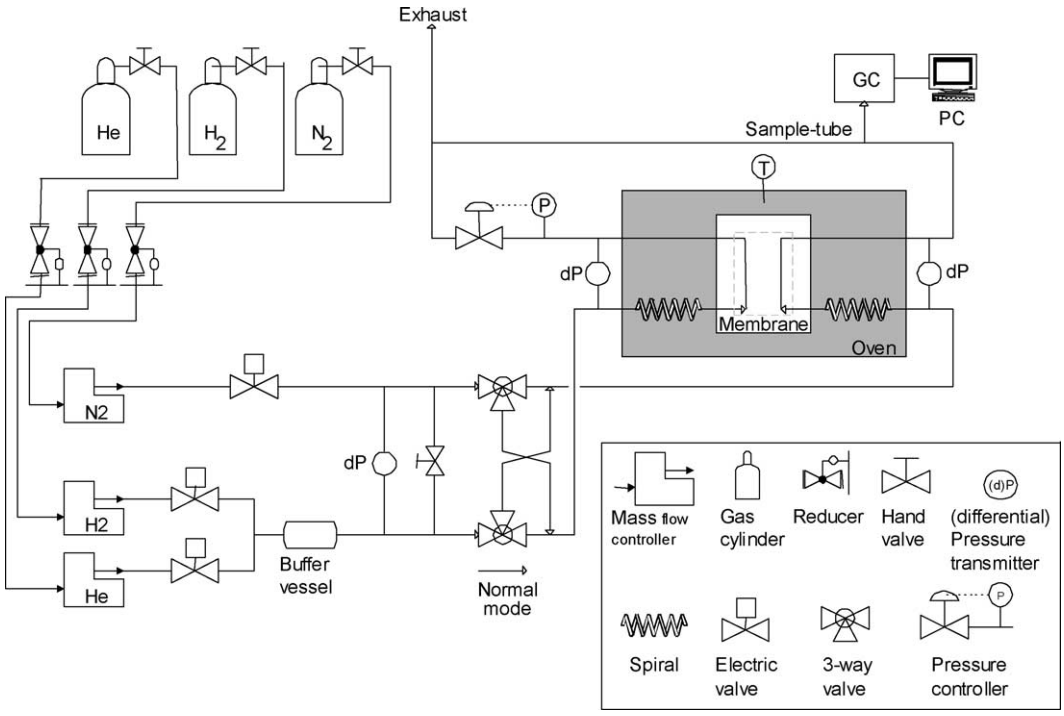

Fig. 7. Schematic drawing of the permeation setup.

and the properties of the membrane modules are summarized in Table 1. After activation (or directly at the start of the measurement if no activation was carried out) pure He was fed to the retentate side and pure N_2 to the permeate side in order to detect any He leak through the membrane. During the leak test a trans-membrane pressure of 50 mbar was applied and four samples were taken. Hydrogen permeation experiments were carried out at 623, 673, and 723 K, respectively, and the H_2 partial pressure in the feed was varied from 0 to 0.83 bar. For each condition, at least four samples were taken at a rate of 4 sample/h.

3. Results and discussion

3.1. Membrane layer characteristics

The membrane thickness as given in Table 1 is derived from the sputtering conditions, but has also been measured by the Dektak surface profiler and by SEM for two membranes. The results of the three methods are in agreement with each other. The composition and homogeneity of the prepared Pd/Ag alloy samples measured by XPS equal the intended concentration of Pd and Ag.

A microsieve-supported membrane without glass packaging has also been examined by SEM. Three different magnifications of the microsieve side are shown in Fig. 8. As can be seen in the SEM pictures, microsystem technology is a highly precise technology, able to produce very uniform perforations. The total perforated area is 20% of the area that covers the apertures. The free membrane surface is approximately 10% larger as a result of under-etching in the SiO_2 layer (Fig. 8C), which has been included in the flux calculation. The free membrane area can be chosen larger but this would have induced large variations in the H_2 driving force along the length of the membrane due to the increase of the H_2 concentration at the permeate side. This would complicate

Table 1
Properties of the various types of fabricated membranes and modules characterized in the permeation setup

Membrane identification	Activated	Forced flow	Thickness (μm)	Microsieve	Composition (wt.%)	
					Pd	Ag
PdAg-ms_1	Yes	No	0.7	Yes	78	22
PdAg-ms_2	Yes	No	0.5	Yes	77	23
PdAg_1	No	No	1.2	No	78	22
PdAg_2	Yes	No	0.7	No	78	22
Pd-ms	No	No	1.0	Yes	100	0
Pd-ff_1	Yes	Yes	1.0	No	100	0
Pd-ff_2	Yes	Yes	1.0	No	100	0
PdTaPd	No	No	1.0	No	Pd(0.2 μm)–Ta(0.6 μm)–Pd(0.2 μm)	

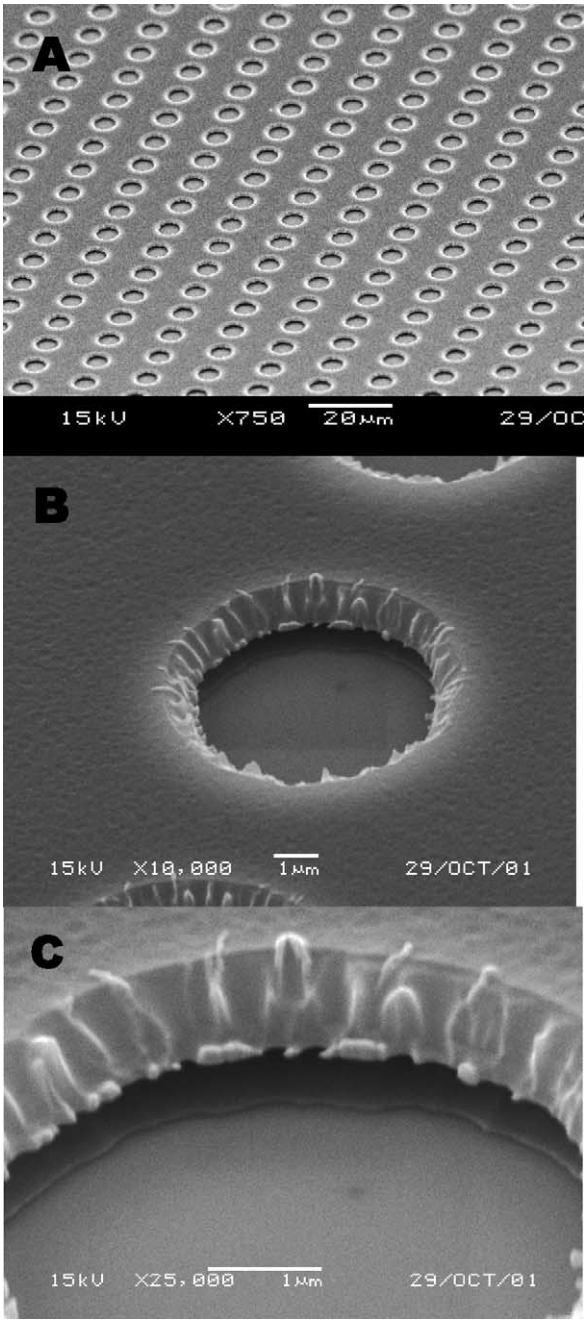

Fig. 8. Three SEM photos of the microsieve with magnifications: (A) 750×, (B) 10,000×, and (C) 25,000×. The extra membrane area created by underetching is clearly visible at photo (C).

the interpretation of the permeation results. In the following, the flux is defined as the molecular hydrogen flow through the membrane divided by the free membrane area.

3.2. Permeation characteristics

In Fig. 9, the measured H_2 flux in time is given for PdAg-ms_1, PdAg_2, Pd-ff_1, Pd-ff_2 and PdTaPd at 0.2 bar H_2 partial pressure in the feed. The fluxes of all membranes appear to increase in time, except for the Pd–Ta–Pd membrane

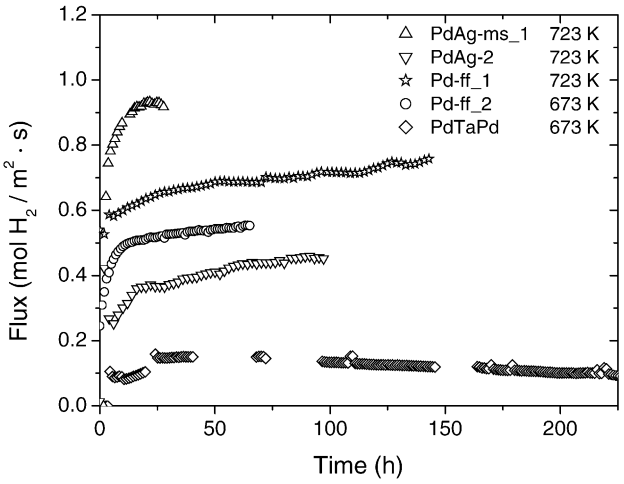

Fig. 9. Hydrogen flux as function of time for different types of membranes and modules. The feed consists of 0.2 bar H_2 and 0.8 bar He.

for which the flux decreases after a slight increase at the start. It seems that the PdAg_2, Pd-ff_1 and Pd-ff_2 still have not reached a steady state after more than 50 h at one process condition. In addition, the H_2 fluxes are rather low with respect to the membrane thickness. Most likely the surface of the membrane was not well activated prior to the shown measurements. A continued activation by H_2 during the measurements reduces the amount of contaminants at the Pd surface, resulting in a flux increase. A further analysis will be made in the next paragraphs. Helium could not be detected in the permeate for the pure Pd and Pd/Ag alloy membrane (Fig. 10), so that the selectivity of membrane Pd-ff_1 and PdAg-ms_1 are in excess of 1500 or 2000, respectively. This indicates that these membranes are pinhole free or close to pinhole free. For the Pd–Ta–Pd membrane, some He could be detected in the permeate almost from the start of the experiment. The He leak increased by a factor of 10 in four steps. We have no explanation yet for the strange combination of decreasing H_2

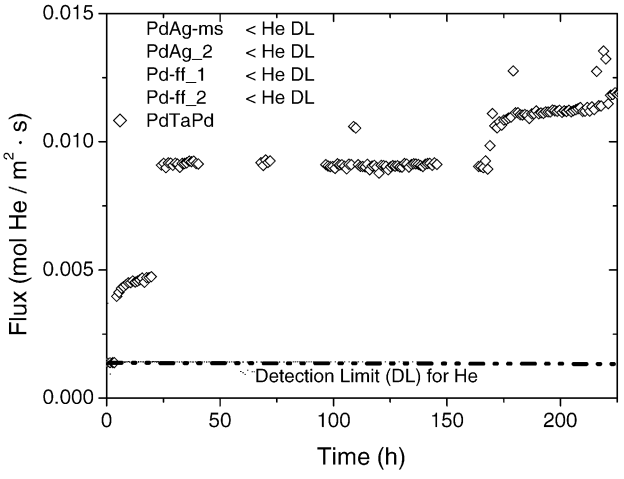

Fig. 10. Helium flux during the same experiments as shown in Fig. 9.

flux and increasing He flux of the Pd–Ta–Pd membrane, but the measurement inaccuracy can be excluded as a cause.

Ward and Dao [9] have presented a permeation model including the various transport steps described in Section 1. Based on this model, a flux of 2.5 mol $H_2/(m^2\,s)$ would have been expected for a 1.0 μm Pd membrane at the conditions used in the experiments, whereas for the Pd/Ag membranes even higher values are predicted. Moreover, from this analysis it would follow that the transport step that limits the H_2 flux is diffusion through the actual membrane layer.

The measured H_2 flux through the membrane can be described by

$$J_{H_2} = P(T)(P^n_{H_2\text{ret}} - P^n_{H_2\text{perm}}) \quad (1)$$

in which J_{H2} is the H_2 flux, $P(T)$ the permeance, and $P_{H_2\text{ret}}$ and $P_{H_2\text{prem}}$ are the H_2 partial pressure at the retentate inlet and permeate outlet, respectively. The value of the exponent n depends on the transport step that limits the hydrogen flux. Based on calculations the mass transfer resistance in the gas phase is excluded as a limiting step. If diffusion through the membrane limits the flux, n will be equal to 0.5 (Sievert's law). If surface reactions at the retentate side limit the flux, n will be unity, whereas when both transport steps are responsible for flux limitations, n will vary between 0.5 and 1.0.

The results of the experiments with varying H_2 concentration in the feed are given in Fig. 11a and b at 673 and 723 K, respectively. The measured flux is plotted against the difference in H_2 partial pressure of the feed inlet and the permeate outlet. From Fig. 11, it can be observed that some spread occurs between the series of ascending and descending H_2 feed concentrations.

To determine which step limits the H_2 transport rate, the measurements with varying H_2 feed concentrations have been fitted to Eq. (1) to obtain the corresponding value of n and the confidence intervals (see Table 2). As expected from the flux behavior presented in Fig. 9 and from the values of the exponent n in Table 2, the permeation through the membrane is mainly limited by H_2 surface reactions. In the case of the Pd membrane, the H_2 permeation is partly limited by the diffusion through the membrane at 723 K (n is smaller than 1), whereas at 673 K the relative influence of diffusion is hardly noticeable (n is close to 1).

In the case of Pd/Ag alloy membranes, a value larger than 1 has been found for n. A possible explanation for this phenomenon could be surface segregation. The occurrence of surface segregation has been found for Pd alloys like Pd/Ni and Pd/Rh [22,23]. Additionally, the adsorption of gasses at the metal surface can influence the degree of segregation [24]. Shu et al. [25] found that the presence of hydrogen in the gas phase will repress the preference of Ag for a location in the surface. Because more Pd will be present at the surface at increasing H_2 partial pressure, more active sites will be available for the necessary surface reactions to adsorb and desorb H_2 from Pd. As a result, the dependency of the flux upon the H_2 partial pressure can be larger than proportional ($n > 1$).

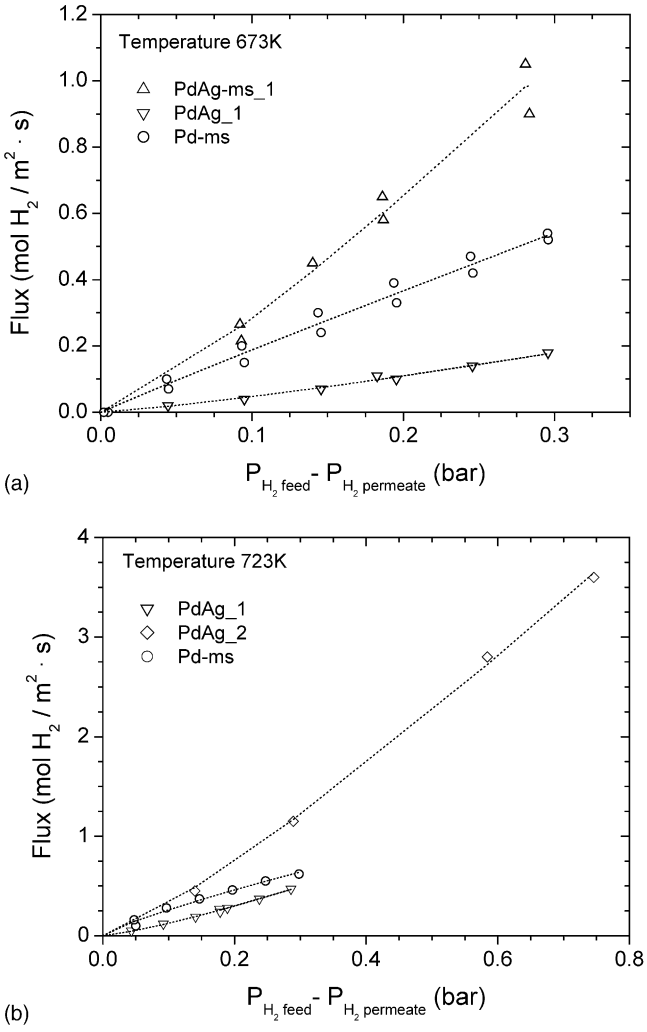

Fig. 11. Hydrogen flux as function of the hydrogen partial pressure in the feed: (a) measurements at 673 K; (b) measurements at 723 K (the lines are to guide the eye).

When the rate determining step remains the same over the temperature range investigated and the number of free active sites for surface reactions remains constant, the temperature dependence of the permeance can be described by an Arrhenius-type of equation:

$$P(T) = C\exp^{-E/RT} \quad (2)$$

in which P is the permeance, C the pre-exponential constant, R the gas constant, T the operating temperature and E is the activation energy of the rate determining step. Eq. (2) implies that a plot of the logarithmic flux values against the reciprocal temperature should result in straight lines. Deviation from a straight line indicates that the activation energy for hydrogen transport changes, i.e. the limiting transport step changes. In Fig. 12, the measured fluxes at 623, 673, and 723 K are plotted against the reciprocal temperature for four membranes. For the pure Pd membrane, the relationship between loga-

Table 2
Permeances and exponents (n) calculated by non-linear regression of the measured data obtained from permeation experiments with varying H_2 partial pressures in the feed and Eq. (1)

Membrane identification	Temperature (K)	Stable flux	Permeance (mol $H_2/(m^2\,s\,bar^n)$)	S.D. (mol $H_2/(m^2\,s\,bar^n)$)	n	S.D.
PdAg-ms_1	673	No	4.15	0.54	1.19	0.11
PdAg_1	673	Yes	0.75	0.09	1.21	0.08
PdAg_1	723	Yes	2.09	0.14	1.23	0.05
PdAg_2	723	No	4.79	0.07	1.20	0.05
Pd-ms	673	Yes	1.74	0.14	0.96	0.06
Pd-ms	723	Yes	1.80	0.14	0.80	0.07

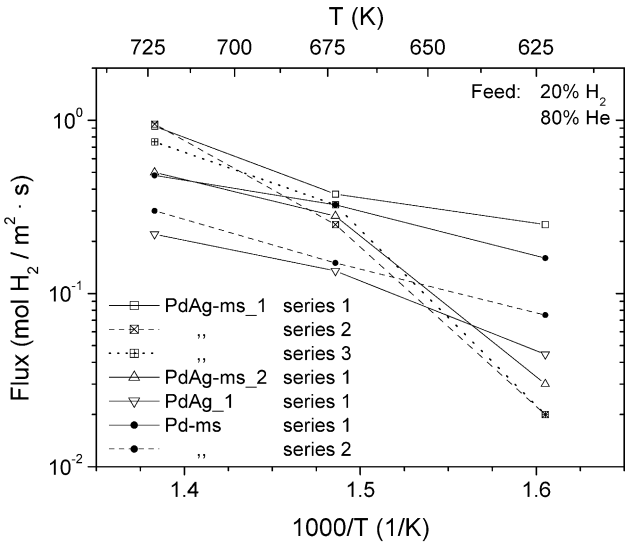

Fig. 12. Hydrogen flux as function of the reciprocal temperature at a feed partial hydrogen pressure of 0.2 bar for different membrane, types and measurement series consecutive in time (the lines are to guide the eye).

rithmic flux and reciprocal temperature is almost linear for both series, unlike most of the measured Pd/Ag membranes, thus indicating that the limiting transport step of the Pd membrane does not change with temperature. The slope variations of the Pd/Ag membranes indicate that the limiting transport step changes with temperature for these membranes. Combining these results with the exponent n as determined above, it is plausible to ascribe the effect of temperature on Pg/Ag membranes to a reduced number of free active sites caused by surface segregation or by surface contamination. Moreover, this effect is so strong that it almost completely overrules the expected diffusion limitation as it is predicted by Ward and Dao model. The effect of segregation can be excluded as cause for the differences between flux values in the consecutive series of PdAg-ms_1, because the equilibrium concentration of Pd and Ag is established in minutes. This is due to the fact that only a few atom layers at the surface are involved in the segregation process [26]. The observed drop in the flux in Fig. 12 between consecutive series is most likely attributed to increased surface contamination. Another indication for surface limitation is that at 723 K the H_2 flux for the 0.7 μm thick PdAg-ms_1 is higher than of the 0.5 μm thick PdAg-ms_2 membrane.

Cleaning the surface with steam or oxygen can provide ways to revert the rate limiting mechanism from H_2 surface reactions to diffusion [27].

3.3. Comparison to literature

In Fig. 13, the permeances of the membranes fabricated with microsystem technology are compared to Pd and Pd/Ag alloy membranes deposited on porous substrates. All permeances are calculated based on $n = 1$. The microsystem-fabricated membranes give the highest permeances, even up to a factor 2.5 higher than for membranes deposited on porous substrates if a membrane area of 25% of the wafer area is taken into account. The permeance increases faster with increasing temperature for the membranes presented in this paper compared to the membranes from the literature. The difference in trend may be caused by the difference in limiting transport step of the H_2 permeance. In our case, the transport is limited by H_2 surface reactions [28], which results in a higher activation energy than if the transport is limited by diffusion through the membrane [29]. Large increments in permeance are still possible for these membranes if the limitation in H_2 permeation can be changed from sur-

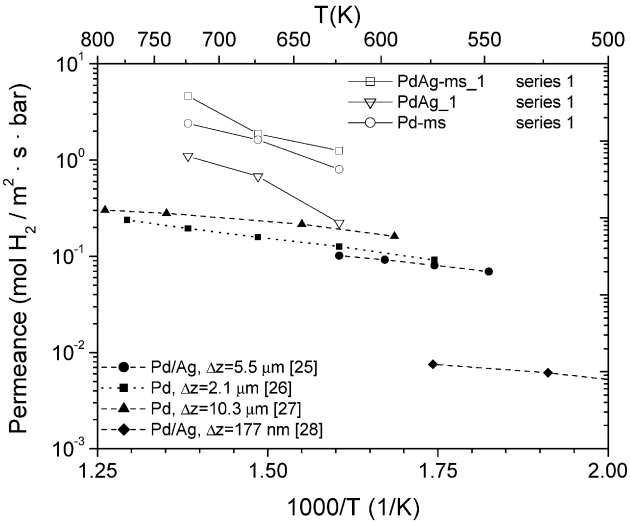

Fig. 13. Comparison of membrane permeances presented in this work with other hydrogen selective membranes deposited on a porous substrate [31–34].

face reaction to diffusion. Thin layers of 200 nm or less are possible, which will theoretically allow for a further increase of the flux by a factor of 4. If the transport limitation cannot be changed from surface reactions to diffusive transport through the membrane, the use of a thinner membrane will hardly improve the H_2 flux. For the microsystem technology-based membranes, the flux limitations due to mass transfer resistances in the gas phase will not be an issue because of the small dimensions of the gas ducts, especially if the flow can be forced through the slits.

Franz et al. [15] and Karnik et al. [30] both measured the flux of a 200 nm thick Pd membrane fabricated with microsystem technology. Franz et al. measured a permeance of 43 mol $H_2/(m^2\,s\,bar)$ at 773 K and Karnik et al. a permeance of 9 mol $H_2/(m^2\,s\,bar)$ at 373 K. Both permeances are higher than the permeances measured for the membranes presented in this paper. Causes are the difference in thickness of the membranes and in case of Franz et al. the operation temperature was higher. Applying n is 0.5 (diffusion limited) instead of 1.0 the permeance measured by Franz et al. agrees with the model of Ward and Dao.

For the membrane of Karnik et al., Ward and Dao predict that the associative desorption would limit the H_2 transport at 373 K. The predicted flux is 1000 times smaller than the one presented by Karnik et al. We have no explanation for this discrepancy.

4. Conclusions

Two different fabrication methods are presented in this paper to prepare high-flux H_2 selective membranes. In both methods, the key factor is the deposition of the metallic layer on a closed and smooth surface layer. Only after deposition of the actual membrane the support is opened to free the membrane surface. This method results in Pd or Pd/Ag alloy membranes free of pinholes, thus exhibiting a high selectivity to H_2. The prepared Pd–Ta–Pd sandwich membrane, however, exhibits some permeance for He. The highest flux has been measured for a 1 μm Pd/Ag membrane with the microsieve support: 3.6 mol $H_2/(m^2\,s)$. Fluxes found in this study are approximately 2.5 times higher compared to membranes deposited on a porous support. H_2 permeation through the Pd membrane appears not only to be limited by diffusion through the membrane but also by H_2 surface reactions. A better activation of the membrane reduces the amount of contamination at the surface, which leads to a higher flux. Eventually, diffusion through the membrane will determine the H_2 flux, which opens the possibility to further improve the flux by applying thinner membranes as shown by Franz et al.

Acknowledgements

This research was supported by the Dutch Science and Technology Foundation (STW), ABB Lummus Global, Aquamarijn and DSM.

References

[1] R.B. McBride, D.L. McKinley, A new hydrogen recovery route, Chem. Eng. Prog. 61 (1965) 81.
[2] Y. Yildirim, E. Gobina, R. Hughes, An experimental evaluation of high-temperature composite membrane systems for propane dehydrogenation, J. Membr. Sci. 135 (1997) 107.
[3] H. Weyten, J. Luyten, K. Keizer, L. Willems, R. Leysen, Membrane performance: the key issues for dehydrogenation reactions in a catalytic membrane reactor, Catal. Today 56 (2000) 3.
[4] E. Kikuchi, Y. Nemoto, M. Kajiwara, S. Uemiya, T. Kojima, Steam reforming of methane in membrane reactors: comparison of electroless-plating and CVD membranes and catalyst packing modes, Catal. Today 56 (2000) 75.
[5] A. Criscuoli, A. Basile, E. Drioli, O. Loiacono, An economic feasibility study for water gas shift membrane reactor, J. Membr. Sci. 181 (2001) 21.
[6] A. Julbe, D. Farrusseng, C. Guizard, Porous ceramic membranes for catalytic reactors—overview and new ideas, J. Membr. Sci. 181 (2001) 3.
[7] R. Dittmeyer, V. Höllein, K. Daub, Membrane reactors for hydrogenation and dehydrogenation processes based on supported palladium, J. Mol. Catal. A 173 (2001) 135.
[8] G. Xomeritakis, Y.S. Lin, Fabrication of thin metallic membranes by MOCVD and sputtering, J. Membr. Sci. 133 (1997) 217.
[9] T.L. Ward, T. Dao, Model of hydrogen permeation behavior in palladium membranes, J. Membr. Sci. 153 (1999) 211.
[10] Y.H. Ma, I.P. Mardilovich, P.P. Mardilovich, Effect of the porosity and pore size distribution of the porous stainless on the thickness and hydrogen flux of palladium membranes, in: Proceedings of the Symposium on Membrane Technology in Petroleum, Petroch, 2001, p. 154.
[11] J.D. Fast, Interactions of Metals and Gases, Macmillan, Eindhoven, 1971.
[12] S. Uemiya, T. Matsuda, E. Kikuchi, Hydrogen permeable palladium–silver alloy membrane supported on porous ceramics, J. Membr. Sci. 56 (1991) 315.
[13] N.M. Peachey, R.C. Snow, R.C. Dye, Composite Pd/Ta metal membranes for hydrogen separation, J. Membr. Sci. 111 (1996) 123.
[14] C.J.M. van Rijn, Membrane Filter and a Method of Manufacturing the Same as well as a Membrane, WO 95/13860, 1994.
[15] A.J. Franz, K.F. Jensen, M.A. Schmidt, Palladium based micromembranes for hydrogen separation and hydrogenation/dehydrogenation reactions, in: Proceedings of the Third International Conference on Microreaction Technology (IMRET3), 1999, p. 382.
[16] C.J.M. van Rijn, M. van der Wekken, W. Nijdam, M.C. Elwenspoek, Deflection and maximum load of microfiltration membrane sieves made with silicon micromachining, J. Microelectromech. Syst. 6 (1997) 48.
[17] H.D. Tong, F.C. Gielens, J.G.E. Gardeniers, H.V. Jansen, W. Nijdam, C.J.M. van Rijn, M.C. Elwenspoek, Microsieve supporting palladium-silver alloy membrane and application to hydrogen separation, J. Microelectromech. Syst., in press.
[18] H.D. Tong, F.C. Gielens, J.W. Berenschot, M.J. de Boer, J.G.E. Gardeniers, W. Nijdam, C.J.M. van Rijn, M.C. Elwenspoek, Fabrication and characterization of MEMS based wafer-scale palladium silver alloy membranes for hydrogen separation and hydrogenation/dehydrogenation reactions, in: Proceedings of the International Conference on Micro Electro Mechanical Systems (MEMS 02), 2002, p. 268.
[19] H.D. Tong, F.C. Gielens, H.T. Hoang, J.W. Berenschot, M.J. de Boer, J.G.E. Gardeniers, H.V. Jansen, C.J.M. van Rijn, M.C. Elwenspoek, A hydrogen separation module based on wafer-scale micromachined palladium–silver alloy membranes, in: Proceedings of the 12th International Conference on Solid State Sensors, Actuators and Microsystems, Boston, 2003, p. 1742.

[20] H.D. Tong, F.C. Gielens, J.W. Berenschot, M.J. de Boer, J.G.E. Gardeniers, W. Nijdam, C.J.M. van Rijn, M.C. Elwenspoek, Microfabrication of palladium–silver alloy membranes for hydrogen separation, J. Microelectromech. Syst. 12 (2003) 622.
[21] F.C. Gielens, H.D. Tong, C.J.M. van Rijn, M.A.G. Vorstman, J.T.F. Keurentjes, High-flux palladium–silver alloy membranes fabricated by microsystem technology, Desalination 147 (2002) 417.
[22] G.N. Derry, C.B. McVey, P.J. Rous, The surface structure and segregation profile of $Ni_{50}Pd_{50}$ (1 0 0): a dynamical LEED study, Surf. Sci. 326 (1995) 59.
[23] J.A. Leiro, M.H. Heinonen, I.G. Batirev, Surface segregation and core-level shift of a Pd–Rh alloy studied by XPS, Appl. Surf. Sci. 90 (1995) 515.
[24] F.J. Kuijers, V. Ponec, The surface composition of Pd–Ag alloys, J. Catal. 60 (1979) 100.
[25] J. Shu, B.E.W. Bogondo, B.P.A. Grandjean, A. Adnot, S. Kaliaguine, Surface segregation of Pd–Ag membranes upon hydrogen permeation, Surf. Sci. 291 (1993) 129.
[26] H.H. Brongersma, Eindhoven, The Netherlands, 2002, personal communication.
[27] F.C. Gielens, R.J.J. Knibbeler, P.F.J. Duysinx, H.D. Tong, M.A.G. Vorstman, J.T.F. Keurentjes, Influence of Steam and CO_2 on the H_2 Flux through Thin Pd/Ag and Pd Membranes, in press.
[28] F.C. Gielens, H.D. Tong, M.A.G. Vorstman, J.T.F. Keurentjes, Extended Characterisation of MEMS-based Hydrogen Separation Membranes, in press.
[29] J. Chabot, J. Lecomte, C. Grumet, J. Sannier, Fuel clean-up system: poisoning of palladium–silver membranes by gaseous impurities, Fusion Technol. 14 (1988) 614.
[30] S.V. Karnik, M.K. Hatalis, M.V. Kothare, Towards a palladium micro-membrane for the water gas shift reaction: microfabrication approach and hydrogen purification results, J. Microelectromech. Syst. 12 (2003) 93.
[31] K. Hou, R. Hughes, Preparation of thin and highly stable Pd/Ag composite membranes and simulative analysis of transfer resistance for hydrogen separation, J. Membr. Sci. 214 (2003) 43.
[32] J. Shu, B.P.A. Grandjean, S. Kaliaguine, A. Giroir-Fendler, J.A. Dalmon, Hysteresis in hydrogen permeation through palladium membranes, J. Chem. Soc., Faraday Trans. 92 (1996) 2745.
[33] A. Li, W. Liang, R. Hughes, Fabrication of dense palladium composite membranes for hydrogen separation, Catal. Today 56 (2000) 45.
[34] B. McCool, G. Xomeritakis, Y.S. Lin, Composition control and hydrogen permeation characteristics of sputter deposited palladium-silver membranes, J. Membr. Sci. 161 (1999) 67.